Influence of Graphite Particle Size and Shape on the Properties of NBR

Jian Yang,[1] Ming Tian,[2] Qing-Xiu Jia,[1] Li-Qun Zhang,[1,2] Xiao-Lin Li[1]

[1]*The Key Laboratory on Preparation and Processing of Novel Polymer Materials, Beijing University of Chemical Technology, Beijing 100029, China*
[2]*The Key Laboratory for Nanomaterials, Beijing University of Chemical Technology, China Ministry of Education, Beijing 100029, China*

Received 24 February 2006; accepted 22 May 2006
DOI 10.1002/app.24844
Published online in Wiley InterScience (www.interscience.wiley.com).

ABSTRACT: Four graphite powder fillers with different form and size were mixed with acrylonitrile butadiene rubber (NBR, acrylonitrile content at 26%) at 20, 40 and 60 phr of the filler loadings, and the obtained compounds were characterized by SEM, tensile test, friction and wear test. Through the SEM observation, it was found that the expanded graphite could not be broken down to small particles uniformly when blended with rubber on the twin-roller. In the tensile test, the graphite with the smallest size possessed the best reinforcement ability as expected. The tribological properties of the rubber were improved when adding more graphite. The largest graphite particles imparted the lowest friction coefficient of the composites among four fillers, but the submicrometer graphite provided the best wear property to NBR.
 J Appl Polym Sci 102: 4007–4015, 2006

Key words: graphite; rubber; mechanical properties; coefficient of friction; wear

INTRODUCTION

Rubber and composite materials are extensively used for radial lip seals of shafts, valve shaft seals, reciprocating piston, and piston rod seals. In those sealing applications, rubber materials are demanded to possess high durability and provide tightness for sealing.[1,2] Most importantly, all dynamic sealing rubber applications require good friction properties: high wear resistance and low coefficient of friction. In sealing applications, NBR, hydrogenated nitrile rubber, acrylic rubber, silicone rubber, and fluorocarbon rubbers are mostly used rubber materials. During the fracture process, basically, the rate of wear appears to depend on how strong the rubber materials are to withstand the friction force, and how big the friction force is.[3,4] Unfortunately, even for the highly reinforced rubber materials, sliding against hard counterface (e.g., metals) in dry contact still cause massive wear, because the friction force will be significant due to the adhesion of rubber to the counterface and the hysteretic property of rubber materials.[5,6] Consequently, various methods have been utilized to lower the friction force and rubber wear,[7–11] for instance, lubrication by oil, surface treatment, bulk modification, and so forth.

Bulk modification is an easy and promising method, attracting more and more interests. The shape and size of the filler particles have great influence on the tribological properties of the polymers. Solid lubricants, such as graphite, molybdenum disulfide, and graphite fluoride, are layered structure and have been incorporated into polymers.[12–15] However, traditional solid lubricants in the size of micrometers are detrimental to the mechanical properties of composites, leading to possible decrease of the wear resistance. Lately nanometer fillers and solid lubricants were employed to improve the tribological and mechanical properties of the polymer composites simultaneously.[16–23] In general, it is believed that the nanoparticles can strengthen the transferred film, and reduce the wear of composites because the fillers have the similar size as the segments of the surrounding polymer chains.[24,25]

As well known, in rubber reinforcement, the most important characteristic for the reinforcing filler is that its size must be small, less than 1 μm, so that the filler particles have large surface area to interact with the rubber.[26,27] Besides the particle size, particle structure and surface chemistry are influential factors in determining the filler's reinforcing efficiency. Fillers are usually made up of primary particles at the smallest size-scale, which are strongly bonded to other primary particles to form an aggregated structure. The aggregates can interact with other aggregates

Correspondence to: X.-L. Li (lixl@mail.buct.edu.cn).
Contract grant sponsor: National Natural Science Foundation of China; contract grant number: 50403029.

through weaker secondary bonding to form agglomerates. After blending, even in perfectly random dispersions of fillers in rubber, there exist many interaggregate physical contacts. The interactions between fillers and rubbers have a significant effect on reinforcement properties of a filled rubber, particularly the filler–filler and filler–rubber interactions.[28,29]

In this study, NBR rubber was chosen as the polymer matrix since it is the most widely and commonly used rubber material for oil sealing applications, and four types of graphite particles with different shape and size were studied as the fillers. Two of them were regular graphite powders, and the smaller one had the thickness in nanometer range. The third one possessed round shape and the fourth one was expanded graphite (EG).[30] When mixing EG with rubber on rollers, the soft and loose structure of EG particle might be broken down to smaller units, and also be compressed to tighter form.

Graphite is a widely used solid lubricant,[31] and graphite filled rubber materials commonly have small compression set.[32,33] In this study, after the graphite fillers were mixed with NBR, the morphologies, mechanical properties, friction and wear properties of the obtained compounds were investigated, for reference to further development of superior rubber composites for sealing applications.

EXPERIMENTAL

Materials

The regular micrometer graphite powder (designated as Micro) and acid intercalated graphite (expansion ratio along *c*-axis is about 200–250 times) were purchased from Pingdu Huadong Graphite Processing Factory, Shandong province, China. Small-sized graphite (referred to as SubM) was bought from Qingdao Huatai Lubricant Sealing Science and Technology Company, Shandong Province, China. Spherical graphite (ab. Spheric) was supplied by QingDao Laixi En-star Graphite Company, China. All of the graphite powders were used as received. NBR rubber, manufacture brand N240S with acrylonitrile content of 26%, was purchased from JSR, Japan. Other ingredients for rubber curing were bought from chemical stores.

Expansion of acid intercalated graphite

Expanded graphite (EG) was prepared by microwave irradiation[34] on the acid intercalated graphite for 1 min in a microwave oven (Sanyo EM-183MS1) with power of 700 W and frequency at 2.45 GHz.

Preparation of graphite filled NBR compounds

Graphite fillers and other ingredients were added to rubber on twin-roller according to the formulation in Table I. In this study, a simple and effective sulfur curing system was selected to avoid interference by other additives and reinforcing fillers. Curing characteristics of the obtained compounds were determined by oscillating disc rheometer (ODR) at 160°C, according to ASTM D2084. Then, the compounds were vulcanized at platen press with 15 MPa pressure at 160°C for the optimum cure time (T_{90}), according to the ODR results.

TABLE I
Formulation for Rubber Compounding

Materials	Amounts (phr)
N240S	100
Sulfur	1.5
ZnO	5
Stearic acid (SA)	1
Anti-aging reagent 4010NA[a]	2
Accelerator DM[b]	1.5
Graphite	Variable

[a] *N*-isopropyl *N*′-phenyl 1,4-phenylenediamine.
[b] Dibenzothiazyl disulfide.

Characterization and tests

Two instruments of scanning electronic microscopes, including a Cambridge (British) S-250MK3 and a high definition XL-30 ESEM of Philips Electron Optics, Netherlands, were used to examine the graphite powders, and the fracture surfaces of the vulcanizates.

Shore A hardness of the vulcanizates were measured according to ASTM D2240, using a XY-1 type A durometer (No. 4 Chemical Machinery Plant of Shanghai Chemical Equipment, Shanghai, China), and three different spots of the sample (over 6 mm in thickness) were measured to give the average. Tensile test were carried out according to ASTM D412. Dumbbell-shaped specimens of the vulcanizates were tested on a CMT4104 testing machine (Shenzhen SANS Testing Machine, Shenzhen, Guangdong province, China), at the speed of 500 mm/min, and five specimens were tested to give the average.

The friction and wear tests were conducted on a MMW1 model friction and wear tester. The contact schematic diagram of the frictional couple is shown in Figure 1. This ring-on-disk sliding couple is carefully designed for the tribology test of rubber-like materials, to improve the repeatability of testing results by avoiding excessive deformation of the soft materials.[7,8] During the tests, the friction force between the test disk and the steel ring was measured with a torque shaft. Sliding was performed under ambient conditions over a period of 1 h at an average sliding speed of 0.1 ms^{-1}. Before each test, the

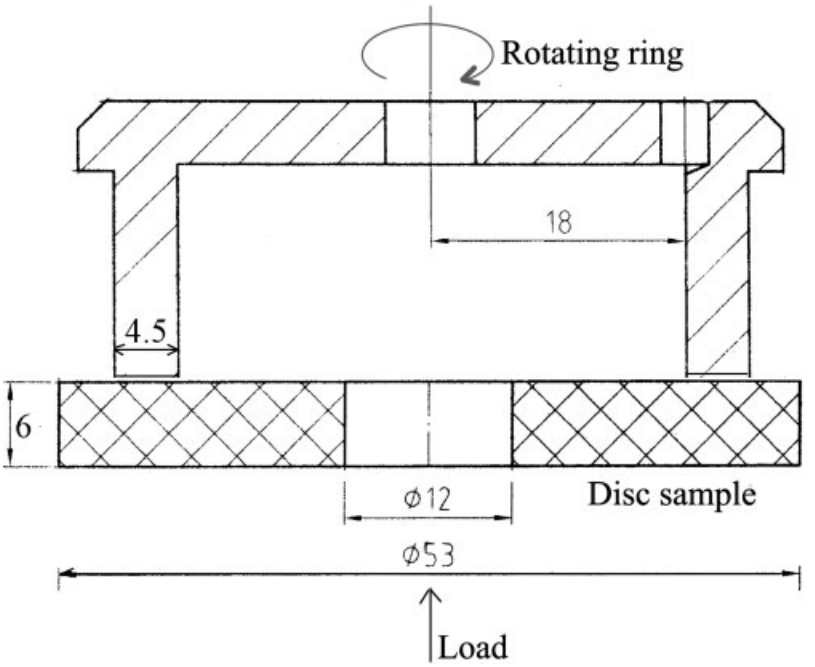

Figure 1 The contact schematic diagram for the frictional couple.

steel ring (45#) was abraded with No. 1000 water-abrasive paper. Then, the steel ring was cleaned with acetone and dried. At the end of each test, the wear weight loss of the sample disk was determined accurately to 10^{-4} g with a high precision analytical balance. Three replicate friction and wear tests were carried out for each specimen to minimize data scattering, and the average is reported in this work. After testing, the morphologies of the worn rubber surfaces were observed with scanning electron microscope.

RESULTS AND DISCUSSION

Structures of graphite fillers

Those four graphite fillers selected in this study are different in size and shape. From Figure 2(a), it can be seen that most of the regular micrometer graphite particles possess the lamellar structure, having the diameter in the range of 5–10 μm and thickness around or above 1 μm. In Figure 2(b), the small-sized graphite (SubM) has the diameter less than 2 μm and thickness in nanometers, for instance, the two marked thickness are around 130 and 157 nm, which is the reason why this type of graphite is referred to as submicrometer graphite in this work. In Figure 2(c), the expanded graphite displays loose and vermicular or wormlike structure after the microwave irradiation on the acid intercalated graphite. Its structure is basically parallel boards, which collapse and deform desultorily, resulting in many pores of different sizes in a wide range, as reported elsewhere.[35,36] The thickness of the graphite sheets on the exfoliated graphite surface seems in nanometer size. The spherical graphite particles exhibit round shape, and have larger size than the regular micrometer graphite, as shown in Figure 2(d).

Size and distributions of the dispersed fillers in the NBR matrix

To investigate the dispersion state of the fillers, SEM was used to observe the vulcanizates' surfaces, which were obtained by either tensile fractured (observed by S-250MK3 SEM) or freeze fractured (by XL-30 ESEM). The scanning electron micrographs are shown in Figure 3. It was found that the distributions of micrometer graphite, SubM graphite, and spherical graphite in rubber were very uniform, while that of expanded graphite was broad. Original EG particles were worms with big size around several hundred microns, as observed in Figure 2(c). When mixing EG with NBR on rollers, the strong shearing force could break them down to smaller units, some of which were in 1–2 μm, but most of others were still in very large size, around 100 μm in diameter and above several microns in thickness. It was believed that on the rollers, EG particles might be pressed from a loose structure to a tight one, in which the size of pores decreased and the intra-particle force became stronger,[37] resulting in big particles which were hard to be broken down in subsequent shearing.

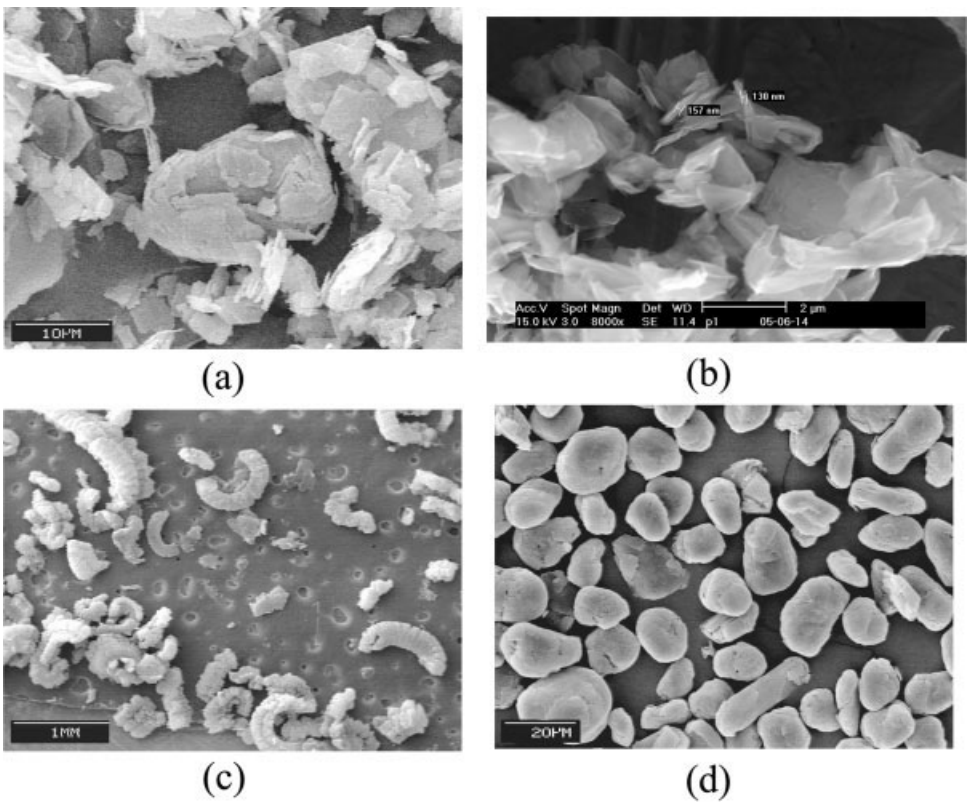

Figure 2 Scanning electron micrographs of the four graphite filler powders. (a) Regular micrometer graphite; (b) submicrometer graphite; (c) expanded graphite; (d) spherical graphite.

According to Figure 3, as expected, the size of dispersed SubM graphite was the smallest among the four fillers, indicating that at the same loading, it would have largest surface area. Figure 3(b–d) reveal that most of the SubM graphite platelets were distributed into very small units, with nanometer thickness. In this size range, the SubM graphite filler studied in this work might provide NBR rubber semireinforcement, quite close to the low surface area carbon black.

Observation on the tensile fractured surface allows one to catch on the interfacial adhesion between the filler particles and rubber matrix. In the SEM micrographs of the micrometer graphite, expanded graphite, or spherical graphite filled NBR, there are clear particle profiles, clear interface boundary, and some cavities caused by detachment of filler particles. That reveals a lack of good interfacial adhesion between either filler with the NBR rubber. For the SubM graphite filled one as shown in Figure 3(b), the interface profiles get indistinct when comparing with the other three, indicating the adhesion is better.

Mechanical properties

Combination of an abbreviation word and a number is designated to each compound in the following discussion. The first part will be Micro, SubM, EG, or Spheric refers to the regular micrometer graphite, the submicrometer graphite, the expanded graphite, and the spherical graphite, respectively. The second one is a number referring to the loading (in phr) of the graphite filler.

The mechanical properties of graphite filled NBR are summarized in Table II. From Table II, it was found that, with each type of filler, the hardness, modulus at certain elongation (e.g., 100%, 300%), and even tensile strength of NBR vulcanizates increased with the increase of filler contents. The elongation at break also increased to some extent when adding more filler. The permanent tensile set became more significant at higher loading.

To compare the effects of different fillers on the tensile properties of NBR rubber at the same loading, Figure 4 shows the typical tensile stress–strain behavior of the vulcanizates filled with the same loading of the four kinds of fillers. As well known, the tests on a tensile specimen provide a fingerprint of a rubber composite, and the resulted data are widely used for quality control and specification purposes. In terms of terminology, tensile stress is the force acting across a unit area in rubber specimen in resisting the separation that tends to be induced by external forces, and strain is the change in length

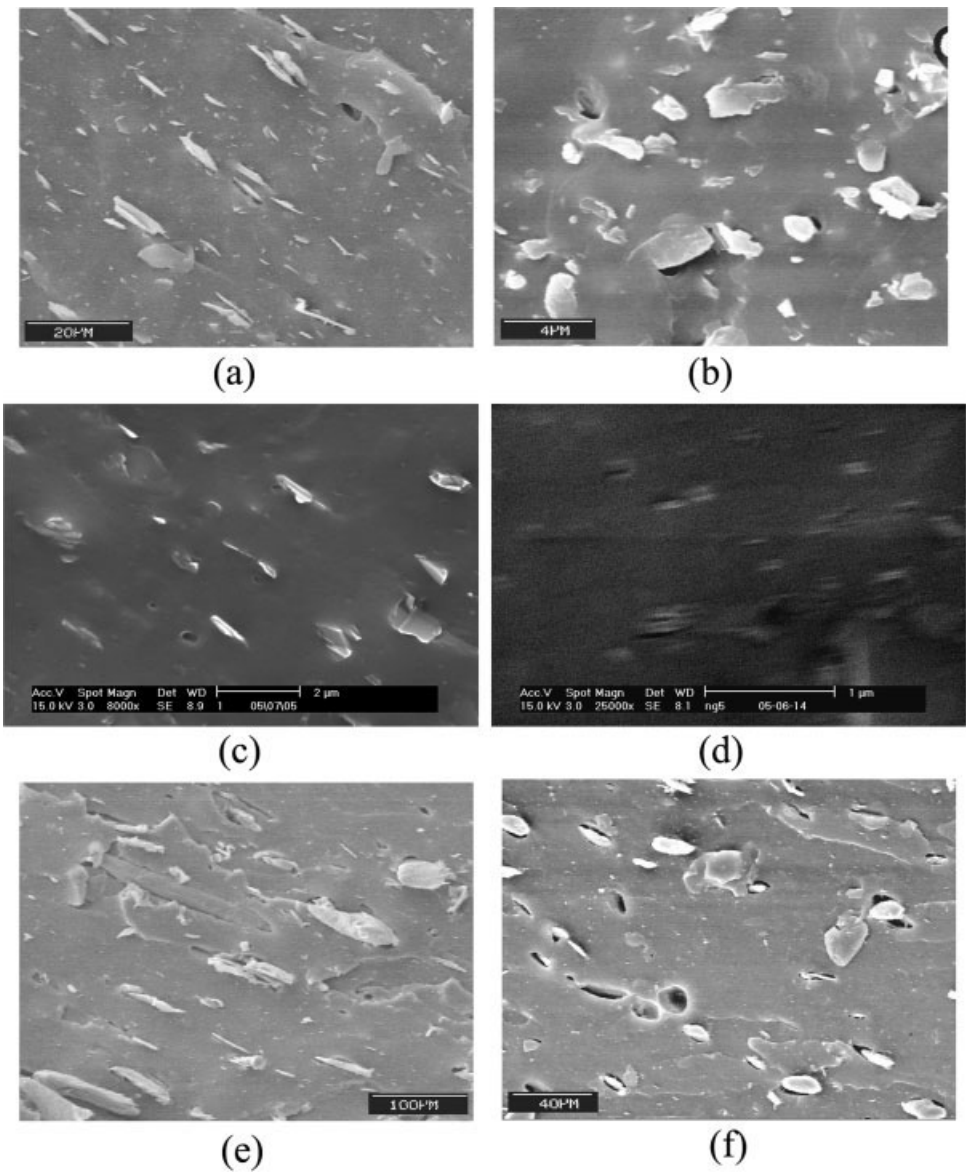

Figure 3 Scanning electron micrographs of the fracture surfaces of vulcanizates. (a) Tensile fracture surface of 10 phr micrometer graphite filled NBR; (b) tensile fracture surface of 10 phr SubM graphite filled NBR; (c) and (d) freeze fracture surface of 10 phr SubM graphite filled NBR; (e) tensile fracture surface of 10 phr expanded graphite filled NBR; (f) tensile fracture surface of 10 phr spherical graphite filled NBR.

of the specimen in tensile direction per unit undistorted length.

From Figure 4, it can be seen that the response of the graphite filled rubber over wide strain range is very nonlinear. For each curve, a Young's modulus (E) could be assigned as the slope of a straight-line tangent to the curve through the origin. As expected, addition of those graphite fillers to NBR rubber increased its Young's modulus. Comparing the Young's modulus of the vulcanizates with different graphite fillers at the same loading, it was found that with expanded graphite was the highest, which was consistent with the results of hardness test since both were measured at low strain. In such a low strain range, bigger filler particles could effectively carried the loaded force. In the previous section, it has been seen that considerable amounts of EG particles dispersed in NBR with quite large size, which is the reason why the vulcanizates with EG possessed the highest Young's modulus. Similarly, those with the SubM graphite had lower Young's modulus than the regular micrometer graphite.

At each loading level, as strain increased, the curve for the SubM graphite filled vulcanizates ascended faster than the others. Particularly at 300% elongation, their stresses are significantly higher. As generally known, the term modulus often is substituted for the term stress at a given elongation. So to speak,

TABLE II
Mechanical Properties of the Graphite Filled NBR

Sample	Shore A Hardness	Modulus at 100% elongation (MPa)	Modulus at 300% elongation (MPa)	Tensile strength (MPa)	Elongation at break (%)	Permanent set (%)
Pure NBR	49	1.0	1.6	3.0	480	4
Micro-10	52	1.2	1.9	3.8	539	10
Micro-20	56	1.7	2.4	4.3	526	16
Micro-30	60	2.5	3.6	7.1	556	28
Micro-40	64	3.1	4.1	8.1	579	40
Micro-60	70	4.6	5.4	9.8	647	60
SubM-10	51	1.2	2.1	3.9	511	8
SubM-20	54	1.6	3.5	5.7	530	12
SubM-30	59	2.1	4.6	8.3	587	24
SubM-40	62	2.7	5.7	8.1	566	26
SubM-60	70	4.3	7.1	10.2	563	40
EG-10	56	1.5	2.0	3.3	488	6
EG-20	61	1.8	2.2	3.0	468	10
EG-40	71	2.6	2.9	5.5	580	30
EG-60	72	2.7	2.8	3.6	529	32
Spheric-10	52	1.1	1.7	2.8	512	6
Spheric-20	56	1.3	1.9	3.9	590	10
Spheric-40	62	1.9	2.6	4.7	614	16
Spheric-60	68	2.8	3.5	5.1	610	28

at same filler contents, the modulus at 300% elongation (M300) of the SubM graphite filled vulcanizate is the highest. One of the main factors affecting the M300 is the crosslinking degree of the vulcanizates, which could be qualitatively described by the ODR test results, listed in Table III. Typical curing curves for graphite filled NBR compounds (40 phr loading) are shown in Figure 5, compared with the unfilled

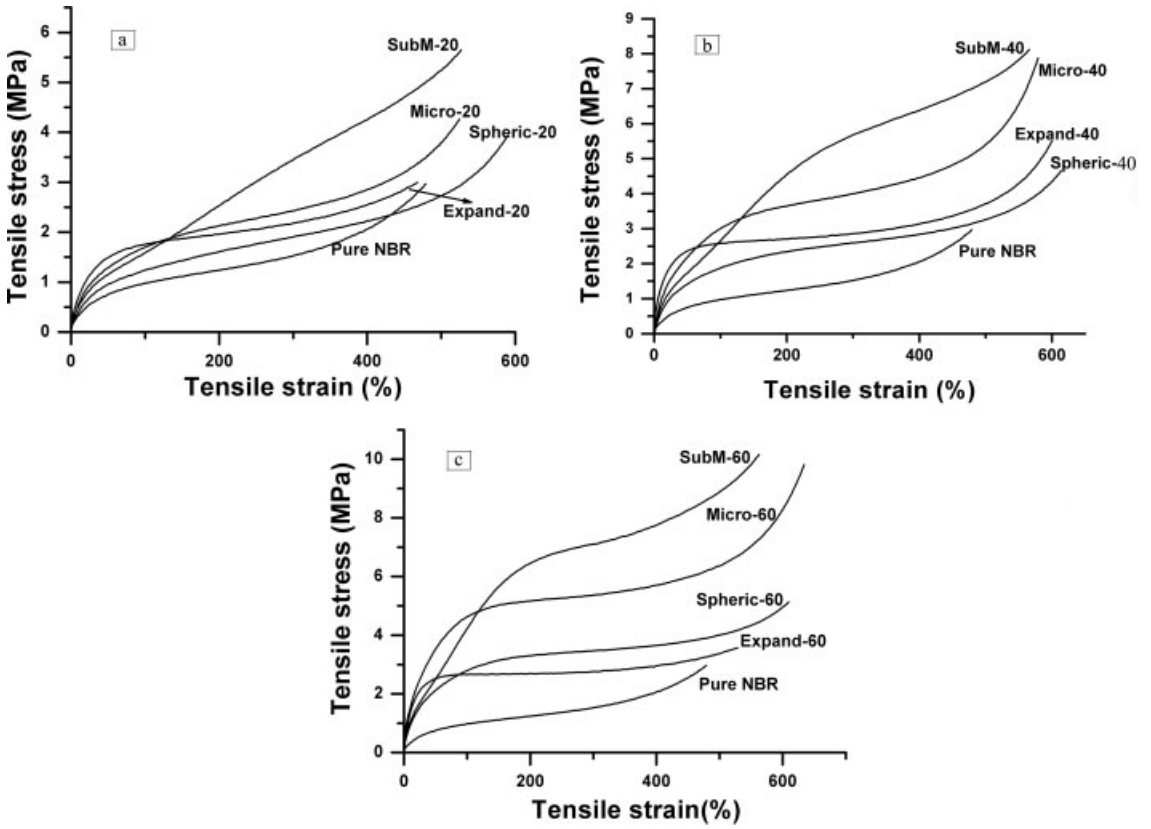

Figure 4 Tensile stress–strain diagrams of the vulcanizates. (a) Filler content at 20 phr; (b) filler content at 40 phr; (c) filler content at 60 phr.

TABLE III
Curing Characteristics of Graphite Filled NBR, Curing on ODR at 160°C

Sample	T_{10} (min:s)	T_{90} (min:s)	Minimum torque (dNm)	Maximum torque (dNm)
Pure NBR	3:35	7:26	5.08	27.21
Micro-20	3:05	6:37	6.66	33.43
Micro-40	2:52	6:56	7.28	36.19
Micro-60	2:30	6:22	8.27	40.28
SubM-20	3:07	7:14	6.05	31.77
SubM-40	2:38	6:01	7.60	35.57
SubM-60	2:43	7:35	8.61	37.19
EG-20	2:53	6:24	5.70	31.66
EG-40	2:44	6:51	6.77	35.42
EG-60	2:34	4:20	9.03	42.60
Spheric-20	3:15	7:10	6.89	33.85
Spheric-40	3:00	6:58	7.61	37.27
Spheric-60	2:45	6:48	8.53	40.76

one. Since the graphite fillers were chemically inert and did not participate in the curing reaction, the curing processes for all of the compounds were quite similar, while addition of the fillers increased the minimum and maximum torques, and also seemed to shorten the scorch time. The change of torque during the curing is directly related to the crosslinking degree of the vulcanizates. From Table III, it can be found that the torque changes of all four kinds of compounds were pretty much the same at each loading level, indicating they were cured to similar crosslinking degree. Therefore, it demonstrated that the dispersion of filler and the interfacial strength between filler particles and rubber matrix were the dominant factors leading to the difference among the M300 of those NBR composites.

When the stress level increases, rubber macromolecular chains at the interface will slide and start to detach from the filler. When the interfacial adhesion is weak, the stress could not be effectively transferred to the filler particles, consequently resulting in a large strain under relatively low stress, for instance, low M300 for the sample EG-40. Based on scanning electron micrographs in Figure 3, the SubM graphite exhibited the best dispersion and smallest dispersed units. That led to the best interfacial strength between the graphite particles and the rubber matrix among all four fillers, virtually resulting in a better transfer of stress from the rubber matrix to filler particles, which contributed to its highest value of M300 among the vulcanizates at each loading level.

Increasing the strain level to rupture shows that the tensile strength of the SubM graphite filled NBR was the highest at each of the graphite content. At the loading of 40 or 60 phr, the tensile strengths of EG or spherical graphite filled NBR were still very low. The main reason is that the interfacial adhesion between big EG or spherical graphite particles and rubber matrix was too weak. When the graphite content increased from 20 to 60 phr, the difference between the tensile strengths of the SubM graphite filled NBR and the regular micrometer graphite

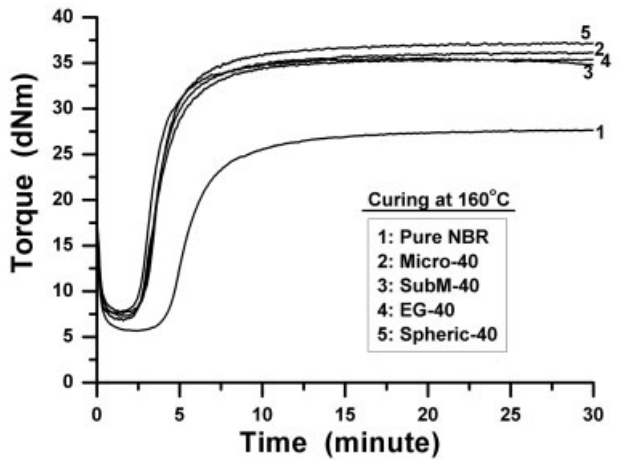

Figure 5 Cure characteristics of 40 phr graphite filled NBR rubber at 160°C.

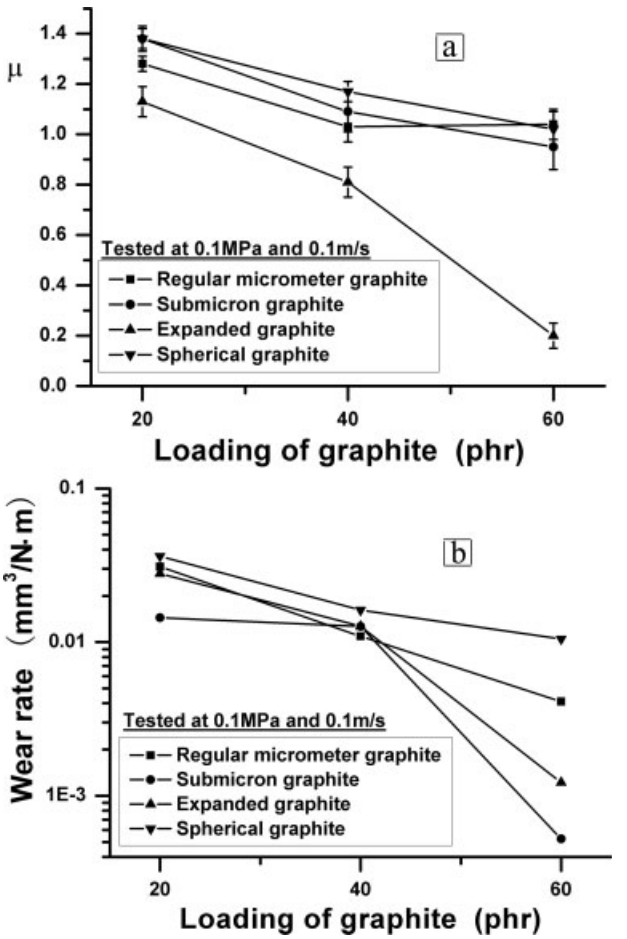

Figure 6 Coefficients of dynamic friction and wear rates of the graphite filled NBR.

filled one became smaller, which can ascribe to the aggregation of the nanofiller and the existence of more microsize particles in the SubM graphite filled ones.

The vulcanizates filled with the graphite having the smallest size, the SubM graphite, appeared to have the best mechanical properties among the four, showing the highest M300 and tensile strength.

Friction test results

The friction coefficient (μ) and wear rate of the unfilled NBR, measured under the same testing condition as comparison, are 1.45 (±0.06) and 0.04 mm^3/Nm respectively, and Figure 6 shows the friction coefficients and wear rates of graphite filled NBR as a function of graphite content. Under the normal pressure of 0.1 MPa and sliding speed of 0.1 m/s, both the friction coefficients and the wear rates decreased gradually with the increasing graphite content for each type of graphite filler. At each loading level, the expanded graphite filled NBR showed the lowest friction coefficient, but they did not have the lowest wear rate. For the other three types, the friction coefficients were pretty much alike at the same filler content. With the graphite content increasing, the wear rate of the SubM graphite filled NBR dropped fast, and at 60 phr, it reached the lowest wear rate in this study. Comparing the sample SubM-60 with EG-60, the former was experiencing larger friction force but wore less, mainly because it had better mechanical properties or antidestruction ability. On the contrary, because the adhesion between the big expanded graphite particles and rubber was very weak, the fillers were easily detached from rubber surface. Similar as EG-60, Spheric-60 showed inferior strength, but it had higher μ value, resulting in quite fast wear rate. Micro-60 had better wear resistance than Spheric-60 mainly attribute to its higher mechanical strength. This confirms that to make better rubber materials for sliding applications under dry condition, both reduction of friction coefficients and reinforcement on mechanical properties are very important. When graphite is filled in NBR as the solid lubricant, smaller size graphite provides better chance to produce the rubber composites with better friction and wear properties.

Figure 7 displays the worn rubber surface after 1-h wear test. In the case of expanded graphite as filler, the graphite flakes evidently orientated parallel to the sliding direction on the surface and covered considerable fraction of the surface, which contributed to its low friction coefficients. The rubber phase was rough after pulling, scratching, and rolling by the counterface, and the interfacial profile between expanded graphite particles and the rubber phase

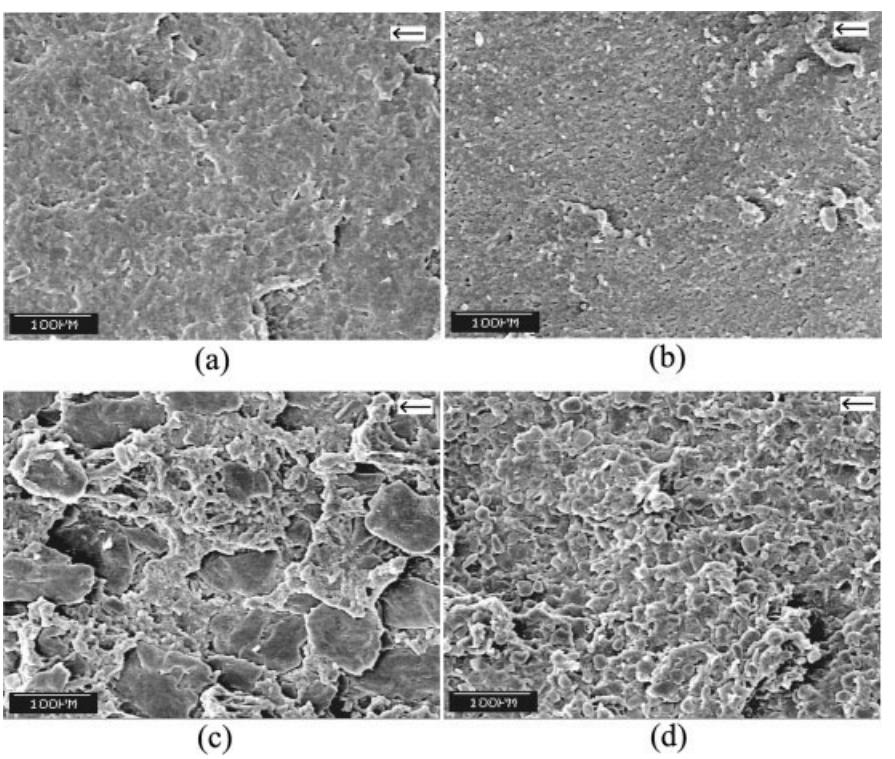

Figure 7 Scanning electron micrographs of the worn rubber surface of the graphite filled NBR, at the graphite content of 40 phr; The arrows point at the relative sliding direction of the rubber surface. (a) Regular micrometer graphite/NBR; (b) submicrometer graphite/NBR; (c) expanded graphite/NBR; (d) spherical graphite/NBR.

was distinct, which confirmed the weak interfacial adhesion. The expanded graphite fillers were easily detached under friction to cause sizeable wear. When the size of the fillers got smaller, the worn surface became smoother. For the SubM graphite, because its size is closest to the dimension of the counterface roughness, the detached filler particles might have a much better chance to adhere on the counterface, which relieve the wear of the composites.

CONCLUSIONS

In this study, four graphite powder fillers with different form and size were mixed with NBR rubber. It was found that expanded graphite could not be uniformly broken down to small particles when blended with rubber on the twin-roller, and thus was not suitable for rubber lubrication using direct mixing process on the rollers. Comparing these four graphite fillers, the graphite with the smallest size possessed the best reinforcement ability, for example, NBR filled with it had the best M300 and tensile strength, lowest permanent set, among all four fillers. Under this study, for each type of graphite, the friction and wear of the composites were reduced with the increase of the graphite content. The largest graphite flake gave the lowest friction coefficient of the composites, but the wear was rather high because of poor mechanical properties. The submicrometer graphite provided better wear property to NBR rubber, though the friction coefficient was still high. It could be expected that rubber materials with excellent mechanical properties and tribological properties would be achieved when the very small sized solid lubricants, or nanometer ones, are well commercialized, and effectively dispersed and uniformly distributed in rubber matrix.

References

1. Stair, W. K. In CRC Handbook of Lubrication (Tribology), Vol. II: Dynamic Seals; Booser, E. R., Ed.; CRC Press: Boca Raton, FL, 1983; pp 581–622.
2. Schweitz, J. Å.; Åhman, L. In Friction and Wear of Polymer Composites; Fredrich, K., Ed.; Elsevier: Amsterdam, 1986; Chapter 9.
3. Gent, A. N.; Pulford, C. T. R. J Appl Polym Sci 1983, 28, 943.
4. Fukahori, Y.; Yamazaki, H. Wear 1995, 188, 19.
5. Schallamach, A. Wear 1971, 17, 301.
6. Barquins, M.; Roberts, A. D. J Phys D: Appl Phys 1986, 19, 547.
7. Bielínski, D. M.; Ślusarski, L.; Affrossman, S.; Hartshorne, M.; Pethrick, R. A. J Appl Polym Sci 1995, 56, 853.
8. Bielínski, D. M.; Ślusarski, L. Wear 1993, 169, 257.
9. Waddell, W. H.; Evans, L. R.; Gillick, J. G.; Shuttleworth, D. Rubber Chem Technol 1992, 65, 687.
10. Patway, R. J.; Maurice Balik, C. Plasmas Polym 1998, 3, 129.
11. Abdrashitov, E. F.; Ponomarev, A. N. High Energy Chem 2003, 37, 279.
12. Bermúdez, M. D.; Carrión-Vilches, F. J.; Martínez-Mateo, I.; Martínez-Nicolás, G. J Appl Polym Sci 2001, 81, 2426.
13. Wang, J. X.; Gu, M. Y.; Bai, S. H.; Ge, S. R. Wear 2003, 255, 774.
14. Yu, L. G.; Yang, S. R.; Liu, W. M.; Xue, Q. J Polym Eng Sci 2000, 40, 1825.
15. Zhang, Z. Z.; Xue, Q. J.; Liu, W. M.; Shen, W. C. J Appl Polym Sci 1999, 72, 751.
16. Su, F. H.; Zhang, Z. Z.; Liu, W. M. Mater Sci Eng A 2005, 392, 359.
17. Rapoport, L.; Nepomnyashchy, O.; Verdyan, A.; Ropovitz-Biro, R.; Volovik, Y.; Ittah, B.; Tenne, R. Adv Eng Mater 2004, 6, 44.
18. Li, F.; Hu, K. A.; Li, J. L.; Zhao, B. Y. Wear 2002, 249, 877.
19. Wang, Q. H.; Xu, J. F.; Shen, W. C.; Liu, W. M. Wear 1996, 196, 82.
20. Ng, C. B.; Schadler, L. S.; Siegel, R. W. Nanostruct Mater 1999, 12, 507.
21. Shi, G.; Zhang, M. Q.; Rong, M. Z.; Wetzel, B.; Friedrich, K. Wear 2003, 254, 784.
22. Zhang, M. Q.; Rong, M. Z.; Yu, S. L.; Wetzel, B.; Friedrich, K. Macromol Mater Eng 2002, 287, 111.
23. Lai, S. Q.; Li, T. S.; Liu, X. J.; Lv, R. G. Macromol Mater Eng 2004, 289, 916.
24. Schwartz, C. J.; Bahadur, S. Wear 2000, 237, 261.
25. Rong, M. Z.; Zhang, M. Q.; Liu, H.; Zeng, H. M.; Wetzel, B.; Friedrich, K. Ind Lubr Tribol 2001, 53, 72.
26. Hamed, G. R. Rubber Chem Technol 2000, 73, 524.
27. Zhang, L. Q.; Jia, D. M. In Symposium of International Rubber Conference; Beijing, China, 2004; Vol. A, p 46.
28. Payne, A. Rubber Chem Technol 1966, 39, 365.
29. Wang, M. Rubber Chem Technol 1998, 71, 520.
30. Chung, D. D. L. J Mater Sci 1987, 22, 4190.
31. Chung, D. D. L. J Mater Sci 2002, 37, 1475.
32. Fegade, N. B.; Phondke, N. A.; Arote, B. R. In 144th Meeting, ACS Rubber Division, October 26–29, 1993 (Paper No. 144).
33. Tang, K. M.; Huang, K. J.; Li, C. Q. Rubber Ind (China) 1995, 42, 723, (in Chinese).
34. Du, X. S.; Xiao, M.; Meng, Y. Z.; Hay, A. S. Polym Adv Technol 2004, 15, 320.
35. Inagaki, M.; Suwa, T. Carbon 2001, 39, 915.
36. Kang, F. Y.; Zheng, Y. P.; Wang, H. N.; Nishi, Y.; Inagaki, M. Carbon 2002, 40, 1575.
37. Celzard, A.; Schneider, S.; Marêché, J. F. Carbon 2002, 40, 2185.